Calculating the Boltzmann Constant Using Johnson Noise

The Ohio State University, Department of Physics, Columbus, OH 43210

Colin Voorhis
Partners: Emily Macbeth, Hirak Basu

Feburary 4th, 2025

Abstract

This experiment analyzes Johnson noise, the random fluctuating voltage produced by the thermodynamic motion of charge carriers in a conducting medium. The RMS of this voltage is recorded for many resistors under a variety of temperatures and bandwidths to approximate the Boltzmann constant, an important proportionality factor in the field of thermodynamics. The Boltzmann constant is found within 2σ of its defined SI value $k_b = 1.380649 \cdot 10^{-23}$ J/K. This experiment also investigates the effects of frequency filters on the effective bandwidth of signal processors.

1 Introduction

Quantized charge carriers such as electrons are able to move inside electrical conductors with some degree of freedom. The motion of these charge carriers is classically based on the the electron gas model, which represents the motion of these charge carriers as a thermodynamic process. The random thermodynamic motion of charge carriers then generates a fluctuating voltage within the conductor. This fluctuation is called Johnson-Nyquist noise, or simply Johnson noise [1].

The RMS of this voltage is proportional to the temperature, frequency bandwidth, and resistance of the system that records it. The RMS voltage is also proportional to the thermodynamic Boltzmann constant k_b which relates the temperature and average thermal energy of a gas. These relationships are applied in fields such as noise thermometry, where the temperature of system can be determined using Johnson noise rather than traditional thermometers [2].

Modern SI standards provide an exact value for the Boltzmann constant in relation to the kelvin [3]. This experiment verifies that definition using RMS voltages generated with a variety of resistance, bandwidth and temperature values.

This experiment also explores how applying high and low pass filters on a signal can have a non-linear impact on the effective bandwidth of that signal.

2 Theory

The voltage fluctuations produced by Johnson noise in a passive resistor relate directly to the Boltzmann constant [1]:

$$\langle V_J^2(t) \rangle = 4 k_B R T \Delta f \tag{1}$$

where:

- $\langle V_J(t) \rangle$ is the RMS of the time-dependent Johnson noise voltage (V)
- k_B is Boltzmann's constant (J/K)
- R is the resistance of the resistor (Ω)
- T is the temperature of the resistor (K)
- Δf is the effective bandwidth of the noise measurement (Hz)

This equation is a classical approximation, but quantum corrections are not required at the temperatures analyzed in this experiment. See Appendix A.1 for a full derivation of this equation and further discussion of its quantum correction.

The voltage signal produced in this experiment is amplified to facilitate its measurement. However, amplifiers also generate voltage noise. These effects can be accounted for as follows [1]:

$$\langle V_J^2(t) \rangle = \frac{V_{out} \cdot 10\,\mathrm{V}}{(G_1 \cdot G_2)^2} - \langle V_N^2(t) \rangle \tag{2}$$

where:

- V_{out} is the recorded voltage, output from the experimental apparatus
- $\langle V_N^2(t) \rangle$ is the time-dependent preamplifier noise
- G_1 is the LLE preamp gain, which is dimensionless
- G_2 is the HLE amplifier gain, which is dimensionless

The HLE amplifier's noise can be neglected in this calculation; only the preamplifier noise requires correction. See Appendix A.3 for more information on amplifier noise.

Δf in this experiment is determined by a minimum frequency f_1 and maximum f_2, which apply low and high pass filters on the signal they receive. The net response of the system $G(f)$ can be approximated as follows [1]:

$$G(f) = \left(\frac{f}{f_1}\right)^2 \cdot \left(1 + \left(\frac{f}{f_1}\right)^4\right)^{-1/2} \cdot \left(1 + \left(\frac{f}{f_2}\right)^4\right)^{-1/2} \tag{3}$$

where:

- $G(f)$ is the filter transmission function
- f_1 is the high pass frequency
- f_2 is the low pass frequency
- f is the frequency passed through the filters

The equivalent bandwidth Δf generated by f_1 and f_2 can be found via the following integral:

$$\Delta f = \int_0^\infty G^2(f) df \tag{4}$$

G(f) can also be determined experimentally by dividing the input and output RMS of a voltages signal passed through these filters. See Appendix A.4 for more information on gain functions.

3 Experimental Methods

3.1 Johnson Noise

Johnson noise is present in nearly all electronic systems, but is most easily detected across a passive electrical component: one with no voltage or current sources acting on it. In this experiment, passive resistors is used to generate Johnson noise data. These resistors are controlled by the Teach Spin Low Level Electronics (LLE), which outputs the voltage signal of one selected resistor at a time. This signal is then amplified and filtered by the High Level Electronics (HLE). The HLE is connected to an oscilloscope and digital multimeter, which are used to record the signal's RMS voltage. See Figure 1 for a visual layout of this apparatus.

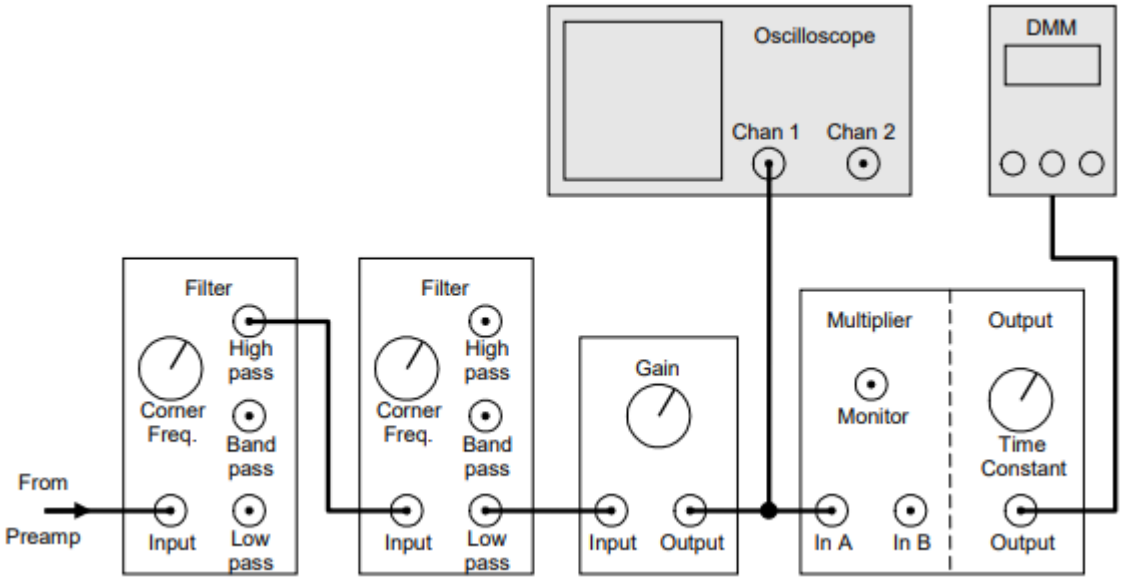

Figure 1: This figure displays a block diagram of the Johnson noise apparatus. The LLE is connected to this system via the cable labeled "From Preamp". It's signal is run through the HLE, which consists of the filter blocks, gain block, and multiplier block connected in series. The resulting output is then fed into the oscilloscope and digital multimeter (DMM). [1]

The resistance, bandwidth, and temperature of the system can all be used to calculate the Boltzmann constant. The output RMS voltage is recorded for many values of each variable while the other two remain constant. Each of these variables has an associated uncertainty, which are discussed in detail in Appendix A.5.1. Overall, the error on bandwidth has the largest impact on fitting parameters.

The HLE's gain G_2 can be varied as needed to scale the output voltage of the system; G_2 is recorded for every recorded set of Johnson noise.

3.1.1 Varying Resistance

The LLE has several built-in resistors, as well as three open resistor slots where external resistors can be installed.

3.1.2 Varying Bandwidth

A variety of f_1 and f_2 values are selected on the HLE to generate different bandwidths.

3.1.3 Varying Temperature

In this case, a peripheral temperature probe is with three resistor slots is used to generate Johnson noise. The probe's temperature can be increased with its internal heater and decreased by submerging it in liquid nitrogen. This probe is attached to the LLE, which then connects it to the rest of the experiment's electronic systems. The voltage of a diode on the probe is used to determine the temperature of the probe as described in Appendix A.2.

3.1.4 Amplifier Noise

The amplifier noise produced by this apparatus can be measured by recording the RMS voltage of the system at a very small resistance $R = 1\,\Omega$. Since Johnson noise is dependent on resistance, but amplifier noise is not, the noise in this signal is almost entirely due to the amplifier [1]. This value is recorded for every combination of temperature and bandwidth used in this experiment. See Appendix A.3 for more information on amplifier noise correction.

3.2 Bandwidth Filters

The effect of the filter frequencies f_1 and f_2 on Δf is also explored in this experiment by driving the filter systems with a sinusoidal signal. A signal generator is configured to output a single-frequency signal and connected to the HLE filters. The pure signal generator output and the filter output are both sent to an oscilloscope. See Figure 2 for a visual layout of this apparatus. The RMS of both signals is recorded. This process is repeated for a variety of signal generator frequencies, as well as several different f_1 and f_2 values.

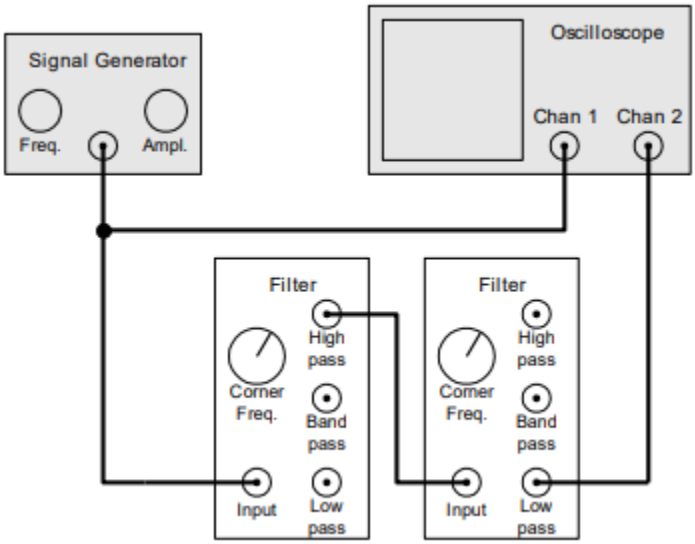

Figure 2: This figure displays a block diagram of the apparatus configured to interface with a signal generator. The signal generator is connected to the HLE filters and the oscilloscope. The HLE filters are also connected to the oscilloscope. [1]

4 Data Analysis and Results

4.1 Johnson Noise

Figure 3 plots resistance against the uncorrected measured voltage and Johnson noise of the system. The error on resistance is found using the known precisions of the LLE for internal resistors and the multimeter for installed resistors. See Appendix A.5.1 for more information on these uncertainties. The linear fit is only calculating using the linear portion of the Johnson noise data.

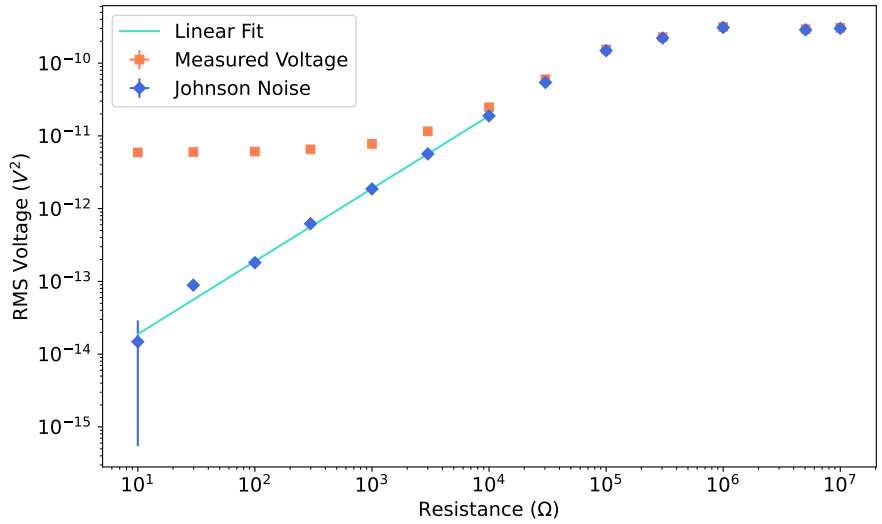

Figure 3: This plots displays the collected RMS voltage and corrected Johnson noise RMS voltage as a function of resistance for $T = 294.2\,\mathrm{K}$ and $\Delta f = 10,996\,\mathrm{Hz}$. The linear fit has $\chi^2/\mathrm{dof} = 2.57$ and approximates the Boltzmann constant as $k_b = 1.444 \pm 0.058 \cdot 10^{-23}\,\mathrm{J/K}$ using a slope of $4k_bT\Delta f$. Error bars are present, but very small, for both axes.

Low resistance measurements here are dominated by amplifier noise. The linear portion of the Johnson noise data is almost entirely contained in this region. Correcting for amplifier noise increases the range of usable resistances by roughly three decades. High resistance measurements are distorted due to capacitive effects in the experimental apparatus. See Appendix A.4 for more information on this distortion. This suggests that extreme values of R are suboptimal for measuring Johnson noise. The two subsequent datasets use a moderate resistance of $R = 10\,\mathrm{k\Omega}$ in part to mitigate these amplifier noise and capacitance effects.

Additionally, this plot verifies the effectiveness of the proposed amplifier noise measurement. For very low resistances, the contribution of Johnson noise to the voltage can be neglected, and the recorded RMS voltage can be considered amplifier noise.

Figure 4 plots bandwidth against Johnson noise. Here bandwidth is calculated using Eq. 4. See Appendix A.4 for more information on this function. All bandwidth values have a 4% uncertainty in measurement. See Appendix A.5.1 for more information on this uncertainty.

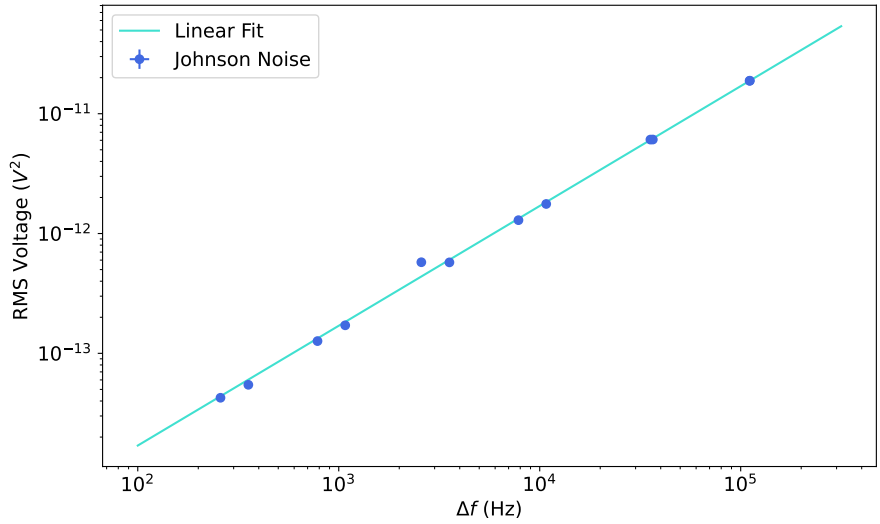

Figure 4: This plot displays the Johnson noise RMS voltage as a function of bandwidth for $R = 10\,\mathrm{k}\Omega$ and $T = 293.8\,\mathrm{K}$. The linear fit has $\chi^2/\mathrm{dof} = 6.01$ and approximates the Boltzmann constant as $k_b = 1.446 \pm 0.044 \cdot 10^{-23}\,\mathrm{J/K}$ using a slope of $4k_bRT$. Error bars are present, but small, for both axes.

Figure 5 plots temperature against Johnson noise. Temperature values are calculated based on the potential difference across a diode in the temperature probe, and their uncertainty is based on the error in this voltage measurement. See Appendix A.5.1 for more information on these uncertainties.

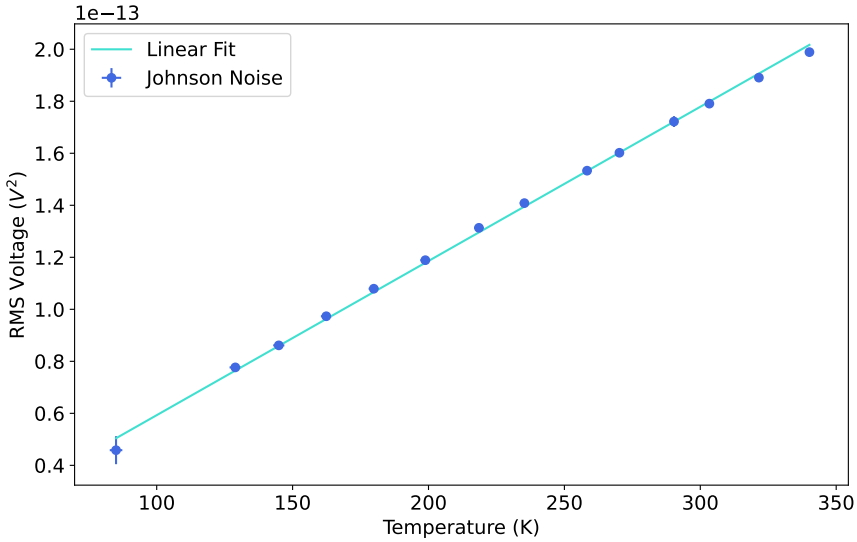

Figure 5: This plot displays the Johnson noise RMS voltage as a function of temperature for $R = 10\,\text{k}\Omega$ and $T = 293.8\,\text{K}$. The linear fit has $\chi^2/\text{dof} = 6.01$ and approximates the Boltzmann constant as $k_b = 1.410 \pm 0.057 \cdot 10^{-23}\,\text{J/K}$ using a slope of $4k_bR\Delta f$. Error bars are present, but small, for both axes.

The residual plots for these data sets are discussed in Appendix A.5.2.

Table 1 summarizes the empirically determined values of k_b for each method, as well as the χ^2/dof of each method's linear fit. Each method gives k_b to within 2σ of its defined SI value $k_b = 1.380649 \cdot 10^{-23}\,\text{J/K}$ [3]. $\chi^2/\text{dof} > 1$ for resistance and bandwidth, suggesting uncertainties are overestimated for these fits. $\chi^2/\text{dof} < 1$ for temperature, suggesting its uncertainties are underestimated.

Independent Variable	Fitted k_b	χ^2/dof
Resistance (Ω)	$1.444 \pm 0.058 \times 10^{-23}$ J/K	2.57
Bandwidth Δf	$1.446 \pm 0.044 \times 10^{-23}$ J/K	6.01
Temperature (K)	$1.410 \pm 0.057 \times 10^{-23}$ J/K	0.66

Table 1: This table displays the value of k_b derived from each method's fitting procedure and each fit's associated χ^2/dof.

Taking a weighted average of the Boltzmann constant generated by each method gives $k_b = 1.434 \cdot 10^{-23} \pm 3.0 \cdot 10^{-25}\,\text{J/K}$. This value is also within 2σ of the defined value of k_b.

The results of this experiment verify the value of k_b and the accuracy of Eq. 1. They also establish a framework for analyzing the effect of low and high pass filters on the effective bandwidth of a signal processor by verifying Eq. 3.

A Supplementary Information

A.1 Johnson Noise

A.1.1 Derivation of Classical Johnson Noise (Eq. 1)

The following derivation is adapted from Boyd's *Radiometry and the Detection of Optical Radiation* [4].

Consider a recently opened circuit with a capacitor of capacitance C and resistor of resistance R connected in parallel. The average energy stored in the capacitor is a function of the voltage $V(t)$ across it:

$$E = \frac{1}{2} C \langle V^2(t) \rangle \tag{5}$$

If we assume that all components are in equilibrium at a given temperature T, the equipartition theorem gives the average energy of the oscillating system as

$$E = \frac{1}{2} k_b T \tag{6}$$

Combining these equations allows us to re-express $\langle V^2 \rangle$ as follows:

$$\langle V^2(t) \rangle = \frac{k_b T}{C} \tag{7}$$

The composition of this voltage can be analyzed using a correlation function $C(\tau)$, which quantifies the causal relationship between the signal and a time-delayed version of itself. $C(\tau)$ is defined as follows:

$$C(\tau) = \langle V(t) \cdot V(t+\tau) \rangle \tag{8}$$

The voltage signal will decrease over time according to an exponential decay based on the circuit's resistance and capacitance:

$$V(t) = V_0 \cdot e^{-t/RC} \tag{9}$$

These two equations can be combined to define $C(\tau)$ as follows:

$$C(\tau) = \langle V(t) \cdot V(t) \rangle e^{-|\tau|/RC} = \langle V(t)^2 \rangle e^{-|\tau|/RC} \tag{10}$$

$C(\tau)t$ can also be related to the spectral density of the voltage $\langle V^2(f) \rangle$ via the Wiener–Khinchine theorem:

$$\langle V^2(f) \rangle = 4 \int_0^\infty C(\tau) \cos(2\pi f \tau) d\tau) \tag{11}$$

Combining Eqs. 10 and 11 allows us to express $\langle V^2(f) \rangle$ as follows:

$$\begin{aligned} \langle V^2(f) \rangle &= 4 \int_0^\infty \langle V^2 \rangle e^{-|\tau|/RC} \cos(2\pi f \tau) d\tau) \\ &= \frac{4 \langle V^2 \rangle RC}{1 + (2\pi f RC)^2} \end{aligned} \tag{12}$$

If we further assume $f << 1/RC$, the equation can be simplified to

$$\begin{aligned}\langle V^2(f)\rangle &= 4\langle V^2\rangle RC \\ &= 4RC \cdot \frac{k_b T}{C} \\ &= 4k_b RT\end{aligned} \tag{13}$$

Spectral density is a measurement of RMS voltage per unit of bandwidth frequency:

$$\langle V^2(f)\rangle = \langle V^2(t)\rangle/\Delta f \tag{14}$$

Substituting this result into Eq. 13 gives the following:

$$\langle V^2\rangle = 4k_b RT\Delta f \tag{15}$$

This is the classical Johnson noise equation shown in Eq. 1. Since it does not relate to C, the previous assumption $f << 1/RC$ can be justified via the limit $C \to 0$.

A.1.2 Quantum Correction

Eq. 13 can be simplified without assuming $f << 1/RC$. Nyquist was able to derive an alternate equation for Johnson noise based on a bounded energy per degree of freedom of $k_b T$ [5]:

$$\text{Energy/Degree of Freedom} = \frac{h\nu}{e^{h\nu/k_b T}} \tag{16}$$

where ν is frequency in place of f, and h is Plank's constant. When $h\nu << k_b T$, this result converges to $k_b T$. Otherwise, this energy factor replaces $k_b T$ in the classical expression, giving the following alternative expression for Johnson noise:

$$\langle V(t)^2\rangle = 4R\Delta f \frac{h\nu}{e^{h\nu/k_b T} - 1} \tag{17}$$

$h\nu << k_b T$ for all achievable combinations of temperature and bandwidth in this experiment, so the classical approximation is sufficient for data analysis.

A.2 Temperature Probe Diode

The temperature probe contains a diode whose voltage is proportional to the probe's temperature. This allows the temperature of the probe to be determined without the use of a thermometer, which would be impractical when the probe is submerged in liquid nitrogen. The TeachSpin manual provides a set of voltages and their corresponding diodes [1]. Figure 6 presents a linear interpolation of this data set designed to establish a relationship between the two values.

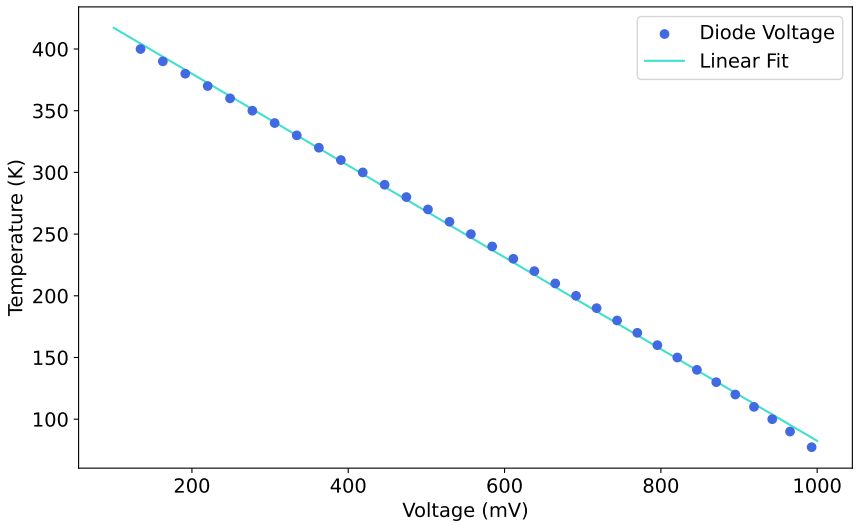

Figure 6: This figure plots diode voltage against the probe temperature that voltage represents. The data is fitted to a line of the form $T = m \cdot V_d + b$. The data is not actually linear, but a linear fit is still able to interpolate between voltage and temperature within an acceptable uncertainty. The parameters of the fit are $m = -0.371 \pm 0.002$ and $b = 454 \pm 1$.

This linear fit gives the following relationship between diode voltage V_d and probe temperature T:

$$T = -0.371 V_d + 454 \tag{18}$$

where V_d is in millivolts, and T is in kelvin.

A.3 Amplifier Noise

A.3.1 Derivation of Amplifier and Noise Correction (Eq. 2)

The voltage signal in this experiment is amplified. This means the measured voltage will be scaled in comparison to the Johnson noise, and some of the signal's noise will be due to the amplifiers. This amplification has several components:

- The LLE contains a preamplifier with a gain $G_1 = 600$.
- The HLE contains an amplifier with a gain G_2. The HLE allows a user to select several discrete G_2 values in the range $[10, 10^4]$.
- The squarer square the voltage is receives, then reduces it by a factor of $10\,\mathrm{V}$.

The resistor will produce a Johnson noise voltage V_J and the amplifiers will produce an more noise voltage V_N. These are related to the voltage output from the squarer V_{out} as follows [1]:

$$\langle V_{out} \rangle = \frac{(G_1 G_2)^2}{10\,\mathrm{V}} \cdot \langle V_J^2 + V_N^2 \rangle \tag{19}$$

This equation can be rearranged to give Eq. 2. V_N is related to the temperature and bandwidth of the system like V_J, but not resistance, because it is generated independently from the resistors in this experiment [1]. This justifies the procedure outlined in Section 3.1.4 for measuring amplifier noise.

A.3.2 LLE vs. HLE Amplifier Noise

Amplifier noise is generated by both the LLE preamplifier and HLE amplifier, but only the noise generated by the LLE requires correction in this lab. This is because the signal is amplified sequentially.

The lowest measurements of Johnson noise in this lab are around $10^{-7}\,\mathrm{V}$. The LLE amplifier generates a RMS noise voltage with roughly the same magnitude, and so effectively doubles the total RMS voltage of the signal. It then scales the signal it receives by a factor of 600. This brings total RMS voltage up to roughly

$$10^{-7}\,\mathrm{V} \cdot 2 \cdot 600 \approx 10^{-4}\,\mathrm{V} \tag{20}$$

The HLE amplifier also produces an RMS noise voltage of order $10^{-7}\,\mathrm{V}$, but that noise is now orders of magnitude smaller than the signal it is amplifying:

$$10^{-7}\,\mathrm{V}/10^{-4}\,\mathrm{V} = 0.001 \tag{21}$$

This means the HLE amplifier's noise will have roughly a 0.1% impact on the voltage of the incoming signal, and can therefore be neglected.

A.4 Gain Function

The behavior of the low-pass filters used in this experiment is effectively modeled by the Butterworth filter response function [1]:

$$G_{low}(f) = \left(1 + \left(\frac{f}{f_c}\right)^4\right)^{-1/2} \tag{22}$$

where f is the input frequency and f_c is a selected "corner" frequency parameter. A similar response equation models the high-pass filters [1]:

$$G_{high}(f) = \left(\frac{f}{f_c}\right)^2 \left(1 + \left(\frac{f}{f_c}\right)^4\right)^{-1/2} \tag{23}$$

This experimental apparatus uses a high-pass corner frequency f_1 and low-pass corner frequency f_2. The effect of both filters together can be modeled by multiplying $G_{high}(f_1)$ and $G_{low}(f_2)$, which gives Eq. 3.

G(f) can be determined experimentally by passing a single-frequency signal through a filter system, and recording its RMS voltage before and after filtering [1]:

$$G(f) = \frac{\text{Input Voltage RMS}}{\text{Output Voltage RMS}} \tag{24}$$

Figure 7 plots the frequency of a signal generator against $G(f)$ values derived from Eq. 24 for $f_1 = 30\,\mathrm{Hz}$ and $f_2 = 33\,\mathrm{kHz}$.

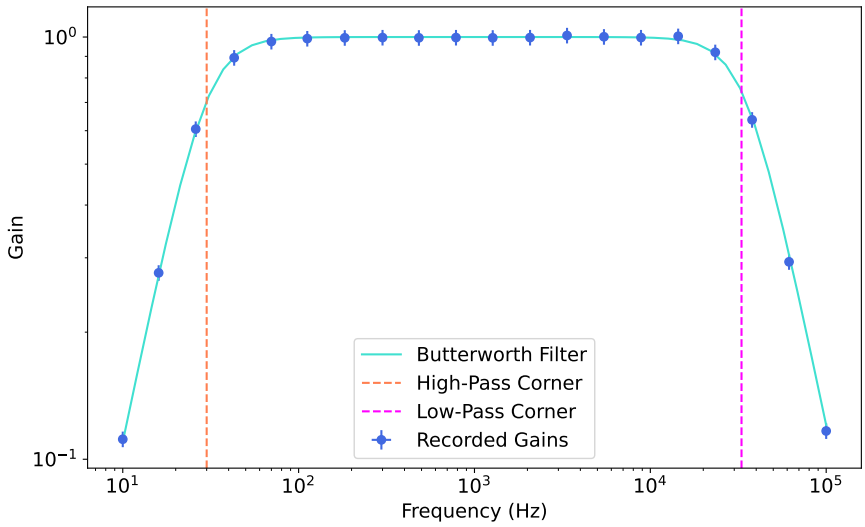

Figure 7: This plot displays recorded gain values as a function of the frequencies used to generate them for $f_1 = 30\,\text{Hz}$ and $f_2 = 33\,\text{kHz}$. Error bars are present for both axes, but too small to view for the horizontal axis.

Figure 8 plots frequency against $G^2(f)$ for $f_1 = 30\,\text{Hz}$ and $f_2 = 33\,\text{kHz}$. The effective bandwidth estimated by the fitted curve can be found using Eq. 4. This specific fit estimates an effective bandwidth of $38700 \pm 400\,\text{Hz}$. The provided effective bandwidth for these filter parameters is $36620\,\text{Hz} \pm 1465$. These two values have overlapping uncertainties at the 2σ level. See Appendix A.5.1 for further information on the uncertainties associated with these values.

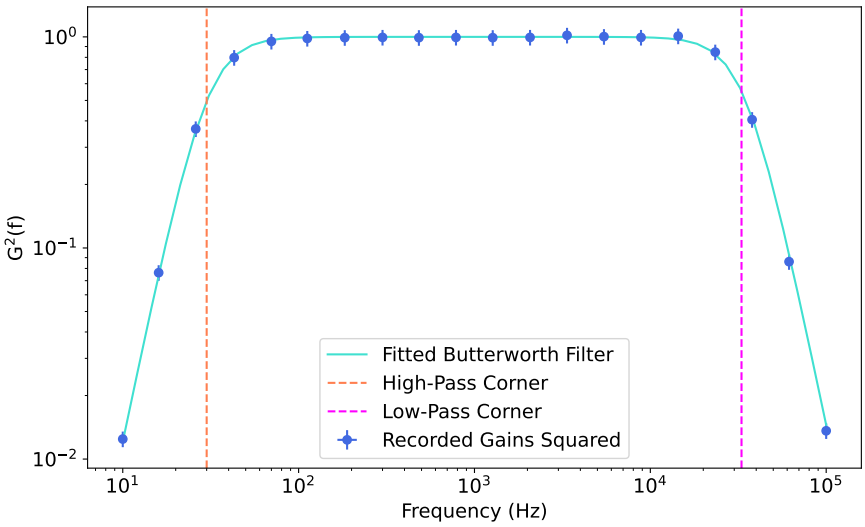

Figure 8: This plot displays squared gain values as a function of the frequency used to generate them for $f_1 = 30\,\text{Hz}$ and $f_2 = 33\,\text{kHz}$. This plot is fitted to the square of Eq. 3. This fit generates the parameters $f_1 = 301 \pm 3\,\text{Hz}$ and $f_2 = 34.8 \pm 0.4\,\text{kHz}$ with $\chi^2/\text{dof} = 0.122$. Integrating this fit according to 4 gives an effective bandwidth of $38700 \pm 400\,\text{Hz}$. Error bars are present for both axes, but too small to view for the horizontal axis.

Per the Teach Spin Noise Fundamentals Manual, this experimental apparatus also experiences capacitive effects that introduce an more low-pass filter with

$$f_c = \frac{1}{2\pi RC} \tag{25}$$

where R is the resistance of the circuit and C is the capacitance of the circuit. $C \approx 10\,\text{pF}$ for local LLE resistors and $C \approx 10\,\text{pF}$ for resistors in the temperature probe. This effect presents an error that is is not mathematically accounted for in the data analysis of this lab. However, resistors with smaller resistances were selected when possible to mitigate this effect. An improved version of this experiment would include a capacitive filter term in all effective bandwidth calculations, especially for measurements taken with the remote temperature probe. [1].

A.5 Uncertainties

A.5.1 Sources of Uncertainty

Resistor uncertainty in this experiment is calculated in two ways. Resistors internal to the LLE are manufacture to a tolerance of $\sigma_R = 0.1\%$. External resistors were measured with a Fluke 175 digital multimeter, which specifies resistance uncertainty σ_R as follows [6]:

$$\sigma_R = \begin{cases} 0.009R + 0.2\,\Omega & R < 600\,\Omega \\ 0.009R + 1\,\Omega & 600\,\Omega \leq R < 6\,\text{k}\Omega \\ 0.009R + 10\,\Omega & 6\,\Omega \leq R < 60\,\text{k}\Omega \\ 0.009R + 100\,\Omega & 60\,\Omega \leq R < 600\,\text{k}\Omega \\ 0.009R + 1\,\text{k}\Omega & 600\,\Omega \leq R < 6\,\text{M}\Omega \\ 0.015R + 10\,\text{k}\Omega & 6\,\text{M}\Omega \leq R < 50\,\text{M}\Omega \end{cases} \tag{26}$$

Effective bandwidth values are derived from the TeachSpin manual, which list an uncertainty $\Delta f = 4\%$ for provided bandwidths.

The temperatures used in the resistance and bandwidth plots were determined using a handheld alcohol thermometer with a precision of 0.1 K.

Diode voltages V_d are measured using the Fluke 175 with uncertainty σ_{V_d} as follows [6]:

$$\sigma_{V_d} = \begin{cases} 0.015V_d + 0.2\,\text{mV} & V_d < 600\,\text{mV} \\ 0.015V_d + 2\,\text{mV} & 600\,\text{mV} \leq V_d < 6\,\text{V} \end{cases} \tag{27}$$

The uncertainty on the probe's temperature σ_T can then be found via propagation of errors:

$$\sigma_T = \sqrt{(V_d^2 \cdot \sigma_{m^2}) + (m^2 \cdot \sigma_{V_d}^2) + \sigma_b^2} \tag{28}$$

The uncertainty on recorded Johnson noise RMS voltages $\sigma_{\langle V_J^2 \rangle}$ is based on the error of the voltage noise $\sigma_{\langle V_N^2 \rangle}$ as follows:

$$\sigma_{\langle V_J^2 \rangle} = \sqrt{\left(\frac{10\text{V}}{(G_1 \cdot G_2)^2} \cdot \langle V_N^2 \rangle\right)^2 + \sigma_{\langle V_N^2 \rangle}^2} \tag{29}$$

The uncertainty on the fitted Boltzmann constant σ_{k_b} is dependent on the method used to calculate it. For a fitted slope value m with uncertainty σ_m, σ_{k_b} for independent resistance is given as

$$\text{Resistance } \sigma_{k_b} = \sqrt{\left(\frac{1}{4T\Delta f}\sigma_m\right)^2 + \left(\frac{m}{4T\Delta f^2}\sigma_{\Delta f}\right)^2 + \left(\frac{m}{4T^2\Delta f}\sigma_T\right)^2} \tag{30}$$

σ_{k_b} is similarly given for independent bandwidth and temperature as follows:

$$\text{Bandwidth } \sigma_{k_b} = \sqrt{\left(\frac{1}{4TR}\sigma_m\right)^2 + \left(\frac{m}{4TR^2}\sigma_R\right)^2 + \left(\frac{m}{4T^2R}\sigma_T\right)^2} \tag{31}$$

$$\text{Temperature } \sigma_{k_b} = \sqrt{\left(\frac{1}{4R\Delta f}\sigma_m\right)^2 + \left(\frac{m}{4R^2\Delta f}\sigma_R\right)^2 + \left(\frac{m}{4R\Delta f^2}\sigma_{\Delta f}\right)^2} \tag{32}$$

Gain values are experimentally measured using an input and output RMS voltage V_{in} and V_{out}, each of which have an error of $\sigma_{V_{in}} = \sigma_{V_{out}} = 3\%$. The error on these gain values $G(f)$ is given as follows:

$$\sigma_{G(f)} = \sqrt{\left(\left(\frac{1}{V_{in}}\right)^2 \cdot \sigma_{V_{out}}\right) + \left(\left(\frac{-V_{out}}{V_{in}^2}\right)^2 \cdot \sigma_{V_{in}}\right)} \tag{33}$$

The uncertainty on the squared experimental gain $\sigma_{G^2(f)}$ can then be determined using propagation of errors:

$$\sigma_{G^2(f)} = 2G(f) \cdot \sigma_{G(f)} \tag{34}$$

The fitting procedure in Figure 8 requires a different propagation of errors for the estimated effective bandwidth Δf, as this bandwidth is calculated based on Eq. 4. This integral does not have a closed form solution, but the uncertainty on the effective bandwidth $\sigma_{\Delta f}$ can be approximating using numerical differentiation of the following equation:

$$\sigma_{\Delta f} = \sqrt{\left(\frac{\partial \Delta f}{\partial f_1}\sigma_{f_1}\right)^2 + \left(\frac{\partial \Delta f}{\partial f_2}\sigma_{f_2}\right)^2} \tag{35}$$

A.5.2 Residual Plots

The residual plots for Figures 3, 4, 5, and 8 are included below. None of the residual plots demonstrate a clear pattern, and all of the residual values lie close to zero. This indicates that the each data set's proposed fitting function accurately reflects its behavior.

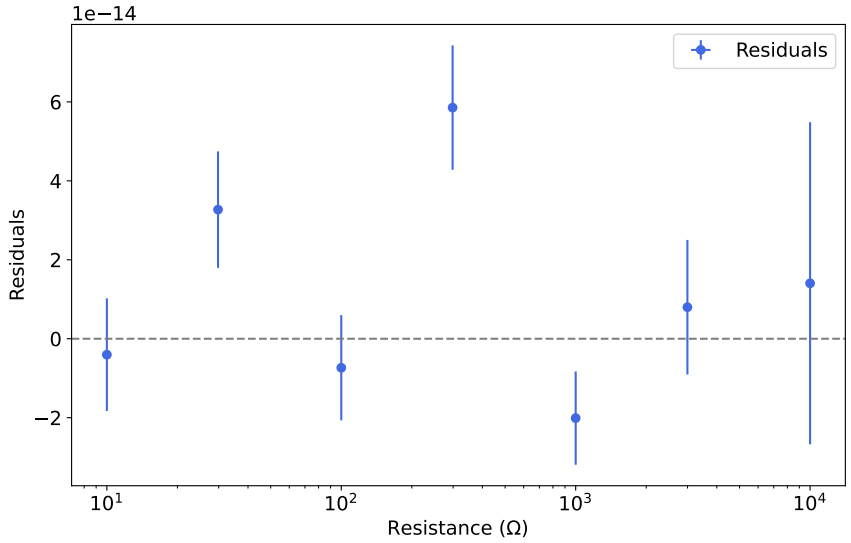

Figure 9: This figure displays the residuals of the resistance vs. Johnson noise data. The residuals show no clear pattern and lie close to zero, indicating that the implemented linear fit accurately models this data set.

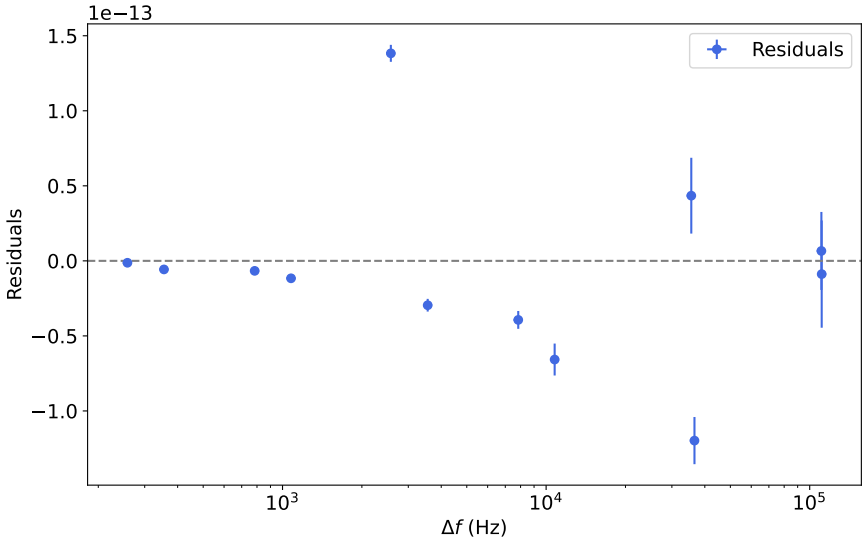

Figure 10: This figure displays the residuals of the bandwidth vs. Johnson noise data. The residuals show no clear pattern and lie close to zero, indicating that the implemented linear fit accurately models this data set.

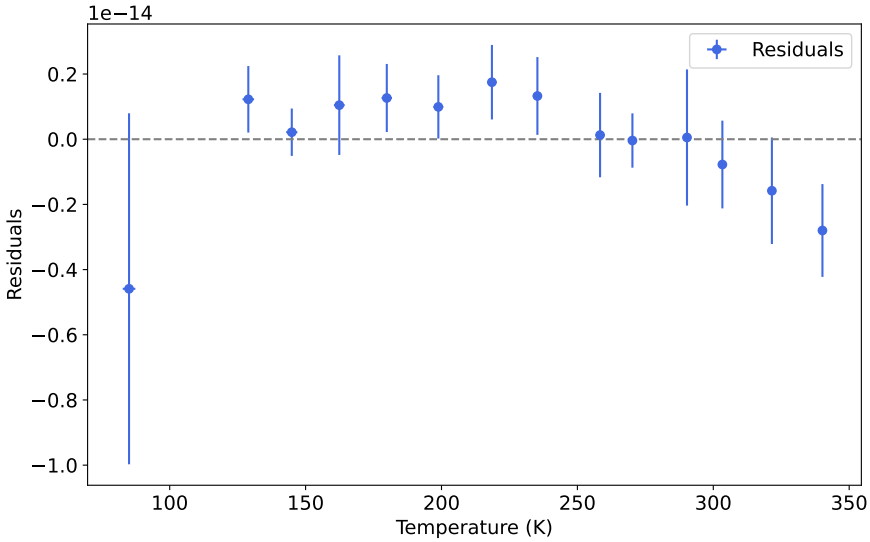

Figure 11: This figure displays the residuals of the temperature vs. Johnson noise data. The residuals show no clear pattern and lie close to zero, indicating that the implemented linear fit accurately models this data set.

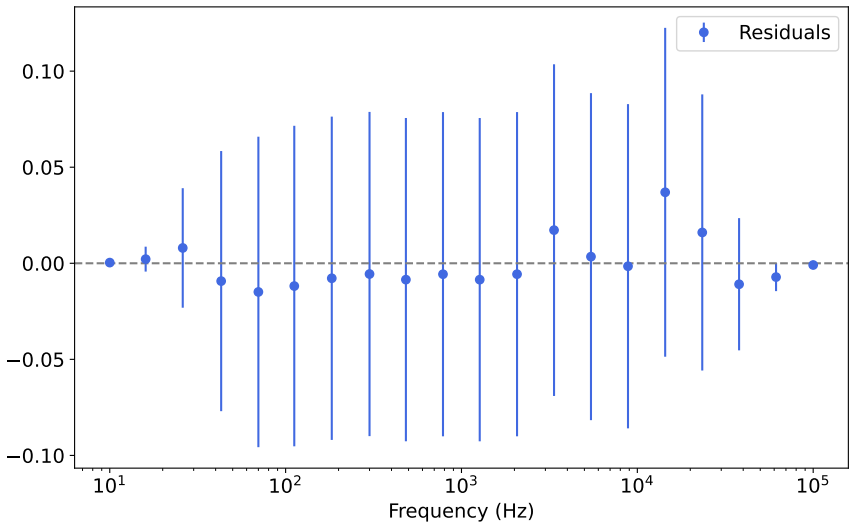

Figure 12: This figure displays the residuals of the frequency vs. $G^2(f)$ data. The residuals show no clear pattern and lie close to zero, indicating that the implemented Butterworth function fit accurately models this data set.

References

[1] David Van Baak. *Noise Fundamentals NF1-A Instructor's Manual*. TeachSpin Inc, 1 edition, 2011.

[2] National Institute of Standards and Technology. Noise thermometry, 2024. Accessed: 2025-02-27.

[3] Bureau International des Poids et Mesures. *The International System of Units 9th Edition (2019)*. Bureau International des Poids et Mesures, 2019. Accessed: 2025-02-27.

[4] Robert W. Boyd. *Radiometry and the Detection of Optical Radiation*. John Wiley & Sons, Inc., New York, 1983.

[5] Harry Nyquist. Thermal agitation of electric charge in conductors. *Physical Review*, 32:110–113, 1928.

[6] Fluke 170 series true-rms digital multimeters. `https://dam-assets.fluke.com/s3fs-public/6011663a-en-17x-ds-w_0.pdf?VersionId=e8AO6eNJpPsAUIhODD5LuxcacBfVJIy9`, 2025.